Chapter 2
Computational Fluid Dynamics Applications in Spray Drying of Food Products

Spray drying is a well-established method for converting liquid feed materials into a dry powder form. It is widely used to produce powdered food, healthcare and pharmaceutical products. Normally, spray dryer comes at the end-point of the processing line, as it is an important step to control the final product quality. It has some advantages, such as rapid drying rates, a wide range of operating temperatures and short residence times. In spray drying operations, CFD simulation tools are now often used, because measurements of air flow, temperature, particle size and humidity within the drying chamber are very difficult and expensive to obtain in large-scale dryer (Kuriakose and Anandharamakrishnan 2010).

2.1 Spray Drying Process

Spray drying is the process of transforming a feed (solution or suspension) from a fluid into a dried particulate form by spraying the feed into a hot drying medium. Spray drying is a widely used industrial process for the continuous production of dry powders with low moisture content (Charm 1971; Masters 1991; Anandharamakrishnan et al. 2007). As shown in Fig. 2.1, spray drying involves four stages of operation: (1) atomization of liquid feed into a spray chamber; (2) contact between the spray and the drying medium; (3) moisture evaporation; and (4) separation of dried products from air stream.

2.1.1 Atomization

Atomization is a process where the bulk-liquid breaks up into a large number of small droplets. The choice of atomizer is most important in achieving economic production of high quality products (Fellows 1998). The different types of atomizer (Masters 1991) are:

C. Anandharamakrishnan, *Computational Fluid Dynamics Applications in Food Processing*, SpringerBriefs in Food, Health, and Nutrition,
DOI: 10.1007/978-1-4614-7990-1_2, © Chinnaswamy Anandharamakrishnan 2013

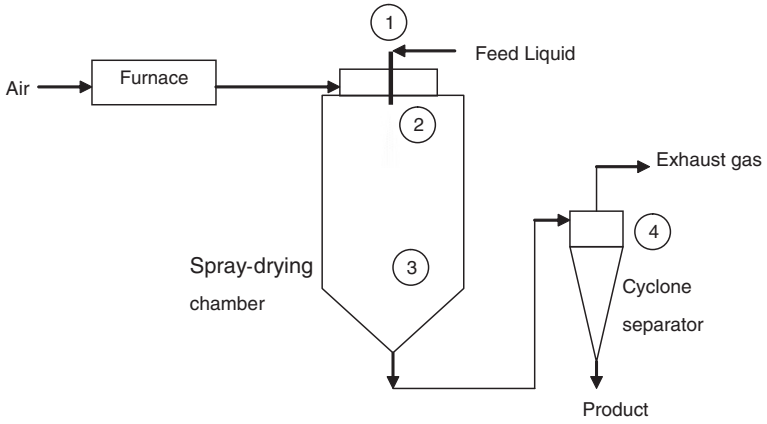

Fig. 2.1 Processing stages of spray dryer

Centrifugal or rotary atomizer: Liquid is fed to the center of a rotating wheel with a peripheral velocity of 90–200 m/s. Droplets are produced typically in the range of 30–120 μm sizes. The size of droplets produced from the nozzle varies directly with feed rate and feed viscosity, and inversely with wheel speed and wheel diameter.

Pressure nozzle atomizer: Liquid is forced at 700–2000 kPa pressure through a small aperture. Here the size of droplets is typically in the range of 120–250 μm. The droplet size produced from the nozzle varies directly with feed rate and feed viscosity, and inversely with pressure.

Two-fluid nozzle atomizer: Compressed air creates a shear field, which atomizes the liquid and produces a wide range of droplet sizes.

2.1.2 Spray–Air Contact

During spray–air contact, droplets usually meet hot air in the spraying chamber either in co-current flow or counter-current flow. In co-current flow, the product and drying medium passes through the dryer in the same direction. In this arrangement, the atomized droplets entering the dryer are in contact with the hot inlet air, but their temperature is kept low due to a high rate of evaporation taking place, and is approximately at the wet-bulb temperature. As the droplets pass through the dryer, the moisture content decreases, the air temperature also decreases, and so the particle temperature does not rise substantially as the particle dries and the effect of evaporation cooling diminishes (Mujumdar 1987). The temperature of the products leaving the dryer is slightly lower than the exhaust air temperature. This co-current configuration is therefore very suitable for the drying of heat-sensitive materials. The advantages of the co-current flow process are rapid spray

evaporation, shorter evaporation time and less thermal degradation of the products (Masters 1991; Anandharamakrishnan et al. 2007).

In contrast, in the counter-current configuration, the product and drying medium enter at the opposite ends of the drying chamber. Here, the outlet product temperature is higher than the exhaust air temperature, and is almost at the feed-air temperature with which it is in contact. This type of arrangement is used for non-heat sensitive products only. In another type called mixed flow, the dryer design incorporates both co-current flow and counter-current flow. This type of arrangement is used for drying of coarse free-flowing powder, but the drawback is that the temperature of the product is high (Masters 1991).

2.1.3 Moisture Evaporation

When droplets come in contact with hot air, evaporation of moisture from their surfaces takes place. The large surface area of the droplets leads to rapid evaporation rates, keeping the temperature of the droplets at the wet-bulb temperature (Mujumdar 1987). In this period, different products exhibit different characteristics, such as expansion, collapse, disintegration and irregular shape. Methods for calculating the changes in size, density and studies of droplet drying are described by Masters (1991).

2.1.4 Separation of Dried Products

The dry powder is collected at the base of the dryer and removed by a screw conveyor or a pneumatic system with a cyclone separator. Other methods for collecting the dry powder are bag filters and electrostatic precipitators (Fellows 1998). The selection of equipment depends on the operating conditions, such as particle size, shape, bulk density, and powder outlet position.

2.2 Types of Spray Dryers

The two main designs of commonly used spray dryers are the short-form and tall-form driers shown in Fig. 2.2.

Tall-form designs are characterized by height-to-diameter aspect ratios of greater than 5:1. Short-form dryers have height-to-diameter ratios of around 2:1. The short-form dryers are the most widely used, as they accommodate the comparatively flat spray disk from a rotary atomizer (Masters 1991). The flow patterns observed in short-form dryers are more complex than those in tall-form dryers, with many dryers having no plug-flow zone and a wide range of gas residence times (Langrish and Fletcher 2001).

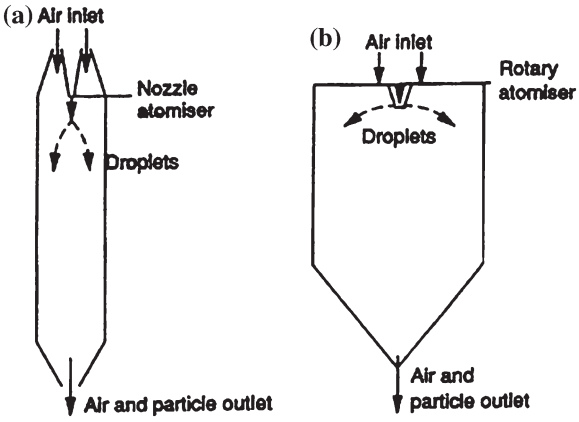

Fig. 2.2 Schematic diagrams of spray dryer (Langrish and Fletcher 2001)

2.3 Airflow Pattern

During spray drying, the particle behaviour is dependent on the air flow pattern. Inside the spray chamber, there is presence of significant air flow instabilities due to the inlet swirl. The various spray drying–air flow studies have been summarized in Table 2.1. Hence, the effect of turbulence inside the spray chamber should be considered. Huang et al. (2004) showed that RNG k-ε model prediction was better for swirling two-phase flow in the spray drying chamber compared to standard k-ε, realizable k-ε and Reynolds stress models.

The air flow patterns in an industrial spray dryer used for milk powder production have been modeled using the transient Reynolds-averaged Navier–Stokes equations with the Shear Stress Transport (SST) turbulence model (Gabites et al. 2010). These simulations were carried out in the absence of atomized liquid droplets. The simulations showed that the main air jet oscillated and processed about the central axis with no apparent distinct frequency. In turn, the recirculation zones between the main jet and the chamber walls fluctuated in size. Good agreement was found between the movements of the main jet via simulations and from telltale tufts installed in the plant dryer. The different outlet boundary condition appeared to have little influence on the overall flow field. In the gas-only simulations, different fluid bed flows within the range had only a local influence by reducing the length of the main jet. This may have an effect on the particle capture by the fluid bed.

2.4 Atomization

The atomization stage during spray drying is very important, since it affects the final particle size. A co-current spray dryer fitted with pressure nozzle was investigated both in experiment and CFD simulation by Kieviet et al. (1996), to develop

Table 2.1 Spray drying–airflow pattern studies (Kuriakose and Anandharamakrishnan 2010)

Problem descriptions	Turbulence model	Findings	Authors
Simulation of airflow pattern with experimental validation.	Standard k-ε and RSM	Non-swirling flow spray chamber; the k-ε model gives good predictions of gas velocity profiles, whereas for swirling flows, RSM model gives better accurate predictions.	Oakley and Bahu (1993)
Simulation of airflow pattern to find out the oscillations in the flow field.	Standard k-ε	Strongest oscillations occur. Good agreement between hot-wire anemometer velocity measurements and simulation results.	Langrish et al. (1993)
Effects of the air inlet geometry and spray cone angle on wall deposition rates.	Standard k-ε	High swirl in the inlet air and large spray cone angle gave the lowest wall deposition rates in both the experiments and simulation.	Langrish and Zbicinski (1994)
Simulation of airflow and particle trajectories in the tall-form dryer with experimental validation.	Standard k-ε	Good agreement between measurements and simulation results.	Zbicinski (1995)
Simulation of airflow pattern, temperature, humidity, particle trajectories and resistance time in a co-current spray dryer fitted with a pressure nozzle.	Standard k-ε	Model prediction agreed well with the experimental measurements of velocity, temperature and humidity.	Kieviet (1997)
Simulation studies on the effects of increased turbulence in inlet airflow.	Standard k-ε	An increase in the amount of evaporation resulted directly from enhanced inlet turbulence.	Southwell et al. (1999)
Temperature and moisture content of the air with the trajectories of the particles.	Standard k-ε	The drying of droplets is influenced by particles surface to surrounding air and diffusion within the particles.	Straatsma et al. (1999)
Investigating the airflow pattern, temperature, velocity and humidity profile at different spray dryer chamber configuration.	Standard *k*-ε	The optimal chamber geometry will depends on the feed properties, atomizer type and drop size distribution	Huang et al. (2003b)

(continued)

Table 2.1 (continued)

Problem descriptions	Turbulence model	Findings	Authors
Experimental and simulation studies of inlet air swirl on the stability of the flow pattern in spray dryers.	RSM	Comparison of with and without spray showed that the introduction of spray has significant effect on the flow behavior. An increase in swirl angle changes the internal flow pattern.	Langrish et al. (2004)
Simulation of a spray dryer with rotary atomizer. Kieviet's (1997) spray dryer geometry was used.	Standard k-ε, RNG k-ε, Realizable k-ε and RSM	Realizable k-ε cannot be used to simulate highly swirling two-phase flow. RNG k-ε turbulent model gives adequate accuracy at reasonable computational time.	Huang et al. (2004)
Simulation of spray dryer fitted with rotary atomizer.	RNG k-ε	More volume of drying chamber is used by rotary atomizer and existence of strong reverse flow just beneath the rotating disc.	Huang et al. (2005)
Simulation of a spray dryer with pressure nozzle and rotary atomizer. Kieviet's (1997) spray dryer geometry was used.	RNG k-ε	Simulation results agreed well with Kieviet (1997) experimental results.	Huang et al. (2006)
Simulation of a spray dryer with rotary atomizer	RANS	Rotary atomizer has a big influence on the flow pattern in pilot scale spray dryer, but its influence decreases with increase in size of spray dryer.	Ullum (2006)
Simulation of industrial scale spray dryer with a new drying kinetics model for a heat-sensitive solution.	Standard k-ε	Good agreement with experimental data. Off-design performance of spray dryer was predicted to analyze the effect of various operating parameters on drying performance.	Huang and Mujumdar (2007)
Evaluation of droplet drying models in a spray dryer fitted with rotary atomizer using CFD simulation	RNG k-ε	The concept of particle rigidity prediction in a CFD simulation was explored, and the effect of initial feed moisture content on the drying models was also studied.	Woo et al. (2008)

(continued)

Table 2.1 (continued)

Problem descriptions	Turbulence model	Findings	Authors
Modeling droplet drying in a spray dryer fitted with a pressure nozzle under steady and unsteady state.	Standard k-ε	2D models can be used for fast and low-resource-consumption numerical calculations with some drawbacks. 3D models can predict the asymmetric flow patterns and provide actual 3D picture of particle trajectories, but require high computing effort.	Mezhericher et al. (2009)
Simulation of industrial scale spray dryer attached with a fluidized bed, using Reaction Engineering Approach (REA).	Standard k-ε	Smaller spray cone angle facilitates easy movement of particles to the fluidized bed. The accuracy of REA model in predicting the single droplet drying kinetics was also explained.	Chen and Jin (2009a)

a theoretical model for the prediction of final product quality. Good agreement was obtained between the experimental data and the simulation. An ultrasonic nozzle spray dryer was studied numerically by Huang et al. (2004). Birchal et al. (2006) simulated a spray dryer fitted with a rotary atomizer for drying of milk emulsion by using CFD, and also by a model with simplified particle motion. Authors also discussed the advantages and limitations of each model in the design and optimization of spray dryers. Studies on the effects of atomizer types (rotary disc and pressure nozzle) on droplet behaviour were performed by Huang et al. (2006) using CFD for spray drying of maltodextrin. They concluded that pressure nozzle may lead to a higher velocity variation in the center of the chamber than the rotary atomizer. Moreover, large recirculation of droplets was also found during pressure nozzle atomization.

2.5 Particle Histories

The understanding of particle histories, such as velocity, temperature, residence time and the particle impact position, are important to design and operate a spray dryer. Moreover, final product quality is dependent on these particle histories. These particle histories can be tracked with the help of CFD simulations.

2.6 Air–Particle Interaction

The primary problem in spray drying modeling is the coupling of equations in mass, momentum and energy between the gas and the droplets. These coupling phenomena of mass transfer from droplet to gas were coupling by evaporation, momentum exchange via drag, and energy coupling by heat transfer, which are schematically shown in Fig. 2.3.

Heat is transferred from the gas phase to the droplets convectively, and this leads to a decrease in temperature of the gas, which it affects the viscosity and density of the gas, which may in turn affect the gas flow field. This also affects the droplet trajectories

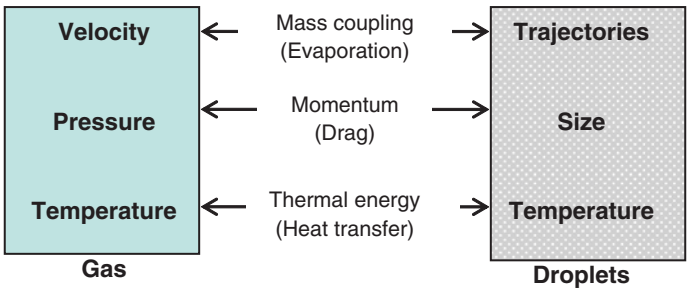

Fig. 2.3 Gas-droplet coupling phenomena

and the heat transfer rate between the droplets and the gas (Crowe et al. 1977). Hence, all three equations (mass, momentum and energy) are interdependent and should be included in the gas-droplet interactions (Kuriakose and Anandharamakrishnan 2010).

2.7 Particle Tracking

Both the Eulerian–Eulerian and Eulerian–Lagrangian methods have been used in published simulations of spray dryings. However, the Eulerian-Lagrangian frame work was selected most often, because it provides residence time of individual particles with a large range of particle sizes. Crowe et al. (1977) first proposed the particle source in the cell (PSI-Cell) model. This is the basis for the discrete phase model (DPM).

In the DPM, the flow field is divided into a grid defining computational cells around each grid point. Each computational cell is treated as a control volume for the continuous phase (gas phase). The droplets are treated as source of mass, momentum and energy inside the each control volume. The gas phase is regarded as a continuum (Eulerian approach), and is described by first solving the gas flow field, assuming no droplets are present. Using this continuous phase flow field, droplet trajectories, together with size and temperature histories along the trajectories, are calculated. The mass, momentum and energy source terms for each cell throughout the flow field is then determined. The source terms are evaluated from the droplet equation and are integrated over the time required to cross the length of the trajectory inside each control volume. The results are multiplied (scaled up) by the number flow rate of drops associated with this trajectory (Crowe et al.1977; Papadakis and King 1988; Fluent 2006). The gas flow field is solved again, incorporating these source terms, and then new droplet trajectories and temperature histories are calculated. This approach provides the influence of the droplets on the gas velocity and temperature fields. The method proceeds iteratively calculating gas and particle velocity fields.

The range of droplet sizes produced by the atomizer is represented by a number of discrete droplet sizes. Each initial droplet size is associated with one trajectory; along with the number of drops it is constant, assuming that no coalescence or shattering occurs. Once the air velocities, temperatures, and humidity are postulated, the transport equations for the droplets of each size are integrated over time and positioned to yield droplet trajectories, velocities, sizes and temperatures. Calculations for droplets of each initial size continue until the volatile fractions (e.g. water) in the droplets evaporate completely, exit the column, or impact the column wall (Papadakis and King 1988; Fluent 2006).

In the CFD simulation, a combined Eulerian and Lagrangian model is used to obtain particle trajectories by solving the force balance equation:

$$\frac{\mathrm{d}\underline{u}_\mathrm{p}}{\mathrm{d}t} = \frac{18\mu}{\rho_\mathrm{p} d_\mathrm{p}^2} \frac{C_\mathrm{D} Re}{24} \left(\underline{v} - \underline{u}_\mathrm{p}\right) + \underline{g} \left[\frac{\rho_\mathrm{p} - \rho_\mathrm{g}}{\rho_\mathrm{p}}\right] \tag{2.1}$$

where $\underline{v}$ is the fluid phase velocity, u_p is the particle velocity, ρ_g is the density of the fluid and ρ_p is the density of the particle.

The particle force balance (equation of motion) includes discrete phase inertia, aerodynamic drag and gravity. The slip Reynolds number (Re) and drag coefficient (C_D) are given in the following equations:

$$Re = \frac{\rho_g d_p \left| \underline{u}_p - \underline{v} \right|}{\mu} \tag{2.2}$$

$$C_D = a_1 + \frac{a_2}{Re} + \frac{a_3}{Re^2} \tag{2.3}$$

where d_p is the particle diameter, and a_1,a_2 and a_3 are constants that apply to smooth spherical particles over several ranges of Reynolds number (Re) given by Morsi and Alexander (1972).

The velocity of particles relative to air velocity was used in the trajectory calculations (Eq. 2.1). Turbulent particle dispersion was included in this model as discrete eddy concept (Langrish and Zbicinski 1994). In this approach, the turbulent air flow pattern is assumed to be made up of a collection of randomly directed eddies, each with its own lifetime and size. Particles are injected into the flow domain at the nozzle point, and envisaged to pass through these random eddies until they impact the wall or leave the flow domain through the product outlet.

The heat and mass transfer between the particles and the hot gas is derived following the motion of the particles:

$$m_p c_p \frac{dT_p}{dt} = hA_p \left(T_g - T_p\right) + \frac{dm_p}{dt} h_{fg} \tag{2.4}$$

where m_p is the mass of the particle, c_p is the particle heat capacity, T_p is the particle temperature, h_{fg} is the latent heat, A_p is the surface area of the particle, and h is the heat transfer co-efficient.

The heat transfer coefficient (h) is obtained from the Ranz-Marshall equation.

$$Nu = \frac{hd_p}{k_{ta}} = 2 + 0.6 \left(Re_d\right)^{1/2} (Pr)^{1/3} \tag{2.5}$$

where Prandtl number (Pr) is defined as follows

$$Pr = \frac{c_p \mu}{k_{ta}} \tag{2.6}$$

where d_p is the particle diameter, k_{ta} is the thermal conductivity of the fluid, μ is the molecular viscosity of the fluid.

The mass transfer rate (for evaporation) between the gas and the particles is calculated from the following equation:

$$\frac{dm_p}{dt} = -k_c A_p \left(Y_s^* - Y_g\right) \tag{2.7}$$

where Y_s^* is the saturation humidity, Y_g is the gas humidity, and k_c is the mass transfer co-efficient and can be obtained from Sherwood number:

$$Sh = \frac{k_c d_p}{D_{i,m}} = 2 + 0.6\,(Re_d)^{1/2}\,(Sc)^{1/3} \tag{2.8}$$

where $D_{i,\,m}$ is the diffusion coefficient of water vapour in the gas phase and Sc is the Schmidt number, defined as follows:

$$Sc = \frac{\mu}{\rho_g D_{i,m}} \tag{2.9}$$

The values of vapour pressure, density, specific heat and diffusion coefficients can be obtained from Perry (1984).

When the temperatures of the droplet has reached the boiling point and the mass of the droplet exceeds the non-volatile fraction, then the boiling rate model is applied (Kuo 1986).

$$\frac{d\left(d_p\right)}{dt} = \frac{4k_{ta}}{\rho_p c_g d_p}\left(1 + 0.23\sqrt{Re}\right) ln\left[1 + \frac{c_g\left(T_g - T_p\right)}{h_{fg}}\right] \tag{2.10}$$

where k_{ta} is the thermal conductivity of the gas and c_g is the heat capacity of the gas (Kuriakose and Anandharamakrishnan 2010).

2.8 Particle Temperature

The particle temperature is very important in the case of heat sensitive products, since it influences the aroma retention and thermal stability of heat labile components. Crowe et al. (1977) predicted that the smaller size particles have higher temperatures than the larger particles, because the latter have a smaller surface area to volume ratio and evaporate more slowly. Kieviet (1997) studied the airflow pattern, temperature, humidity, particle trajectories and residence time in a 2D co-current spray dryer fitted with a pressure nozzle using maltodextrin as feed solution, and concluded that the gradients in the center region of the drying chamber could be improved. Anandharamakrishnan et al. (2010a) studied the particle temperature in both short-form and tall-form spray dryer using CFD simulation for drying of whey proteins. They found that due to moisture evaporation of droplets, the temperature of droplets was high and was almost equal to the gas temperatures outside the core region. Moreover, the temperature of gas in the core spray region and the upper part of the chamber decreased due to the cooling effects of evaporation. The particle nature was also affected by the outlet air temperature (Kuriakose and Anandharamakrishnan 2010).

2.9 Residence Time of Particle

The particle residence time has a great impact on the final powder quality and it also affects product qualities such as solubility and bulk density. The residence time (RT) is divided into two parts; namely, primary and secondary residence times.

The primary RT is calculated from the time taken for droplets leaving the nozzle to impact on the wall or leave at the outlet. The secondary residence time can be defined as the time taken for a particle to slide along the wall from the impact position to the exit (Kuriakose and Anandharamakrishnan 2010).

Kieviet and Kerkhof (1995) determined the RTD of particles in a co-current spray dryer during the drying of aqueous maltodextrin solutions. Kieviet (1997) observed that during spray drying of maltodextrin solution, the larger diameter particles have longer RTs than smaller particles. He also found enormous difference between measured and predicted results due to particle wall depositions and sliding movement. Ducept et al. (2002) performed an experiment to determine the RTD of particles, and validated with the CFD predictions in a superheated steam spray dryer. The residence time distribution of different sized particles in a spray dryer was studied by Huang et al. (2003a), and they found that different droplets follow different trajectories in the drying chamber.

Anandharamakrishnan et al. (2010a) studied Particle Residence Time Distribution of whey proteins in both short-form and tall-form dryers and the residence time (Fig. 2.4). The study indicates that most of the particles have very low RT during spray drying (short-form). It was observed that a bent outlet pipe inside the chamber increases gas and particle recirculation (Fig. 2.4); consequently, cold gas is mixed with down-flowing hot inlet gas, and dried particles will be exposed to the high inlet gas

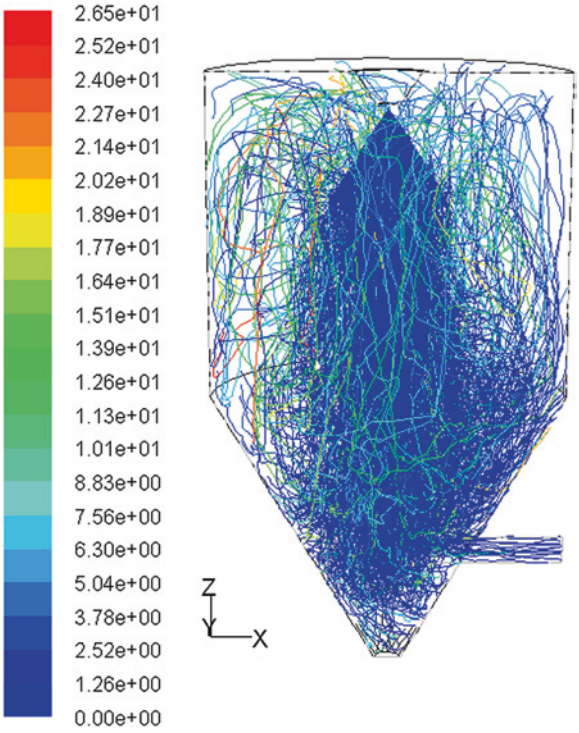

Fig. 2.4 Particle trajectories colored by residence time(s) (Anandharamakrishnan et al. 2010a)

temperatures. This recirculation may lead to denaturation of proteins or inactivation of enzymes. Hence, bend outlet pipe needs to be avoided inside the chamber for producing high quality spray dried food products. Moreover, they found a large difference between the gas and particle residence time. However, there is no direct measurement of primary RT available to confirm the predictions, and this is an interesting challenge for future research (Kuriakose and Anandharamakrishnan 2010).

2.10 Particle Deposition and Position

The knowledge of particle impact positions is important for the design and operation of spray dryers, as it influences the final product quality. In an earlier numerical study, Reay (1988) has shown that the most likely areas for wall deposition are an annular area of the dryer roof and a region below the atomizer, where large particles are likely to deposit. Later, Kieviet (1997) investigated the interaction of wall deposition with the residence time, and the effect of wall deposition on the product quality and yield during spray drying of maltodextrin. Goula and Adamopoulos (2004) determined the operating conditions that influence the fouling and residue accumulation of the equipment during the drying process. Anandharamakrishnan et al. (2010a) studied the particle impact position during drying of whey proteins from the simulation data using an in-house post-processor. Figure 2.5a, b shows the top and front cross-sectional views of the simulated results (Anandharamakrishnan et al. 2010a). Figure 2.5a, b indicates that a large fraction of the particles (50 %) strike the conical

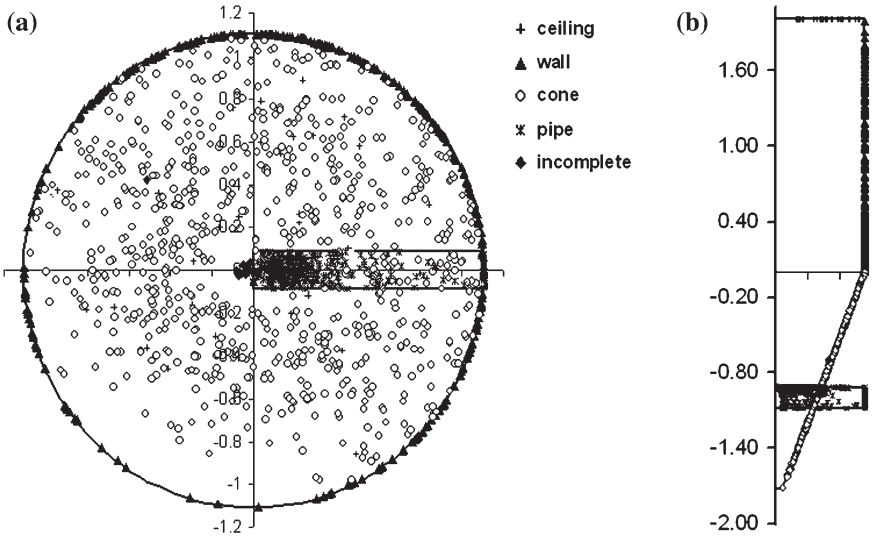

Fig. 2.5 Particle impact positions, **a** top view, **b** front view (Anandharamakrishnan et al. 2010a)

part of the spray dryer chamber (similar with the earlier observation of Langrish and Zbicinski 1994) and 23 % of particles hit the cylindrical part of the wall, but only a small proportion (25 %) of the particles come out of the outlet pipe line (the intended destination). A very small 2 % of particles hit the ceiling despite the large volume of re-circulated gas, but particles hitting the cone and/or cylindrical wall (73 %) should slide down to the main outlet aided by mechanical hammer operations. They also found that in a short-form dryer, a large fraction of the particles strike the conical part of spray dryer chamber, while in tall-form dryer, the particles struck the cylindrical part of the wall. In both forms of dryer, they found less impact on the ceiling, despite the recirculation of gas in the zone (Kuriakose and Anandharamakrishnan 2010).

2.11 Current Trends

In recent years, application of the Reaction Engineering Approach (REA), drying kinetics model, droplet–droplet interactions, unsteady state modeling and population balance model for the simulation of spray dryers has been increasing. The Reaction Engineering Approach assumes that evaporation is an activation process to overcome an energy barrier, while this is not the case for condensation or adsorption. The basic concept of REA was described by Chen and Xie (1997) and Chen et al. (2001). This method describes the droplet drying trend, giving a detailed account of the temperature changes that occur within the droplet during the drying period; some experimental data are required to determine the model parameters. The REA model was used by Chen and Xie (1997) for the simulation of drying of thin-layer food materials such as kiwifruit, silica gel, potato and apple slices. Moreover, Huang et al. (2004) found that this approach (REA) fits in well with the fluent commercial CFD code for spray drying.

The experimental determination of spray drying kinetics was performed by Zbicinski et al. (2002). They determined the spray drying kinetics as a function of atomization ratio and drying agent temperature. They also proved that, based on the critical moisture content of the material, spray drying kinetics can be determined from the generalized drying curves. These lab-scale details can be used for scaling up the spray drying process. Further, Woo et al. (2008) analyzed the effect of wall surface properties on the deposition problem during spray drying using different drying kinetics. They concluded that proper selection of dryer wall material will provide potential alternatives for reducing the deposition problem. Roustapour et al. (2009) performed a CFD study for the drying of lime juice. They determined the drying kinetics based on experimental results of moisture content variation along the length of chamber, and numerically estimated residence time of droplets. The authors found that an increase in initial droplet diameter resulted in a lower particle residence time. CFD was used to gain more insights into the drying characteristics of the mono-dispersed droplets produced using a low velocity spray tower. Introduction of droplet and mass transfer did not significantly alter the flow field. Analysis revealed that the wet bulb region was significant in this tower.

Varying the inlet air temperature from 100 to 180 °C resulted in contrasting drying histories. These drying kinetics were then extended to assess the in situ crystallization phenomenon. For this spray drying tower, it was found that lower inlet temperature conditions favored a higher degree of crystallinity.

Droplet–droplet interactions during the spray drying were performed by applying the transient mode of calculations (Mezhericher et al. 2008). The droplet collisions influenced the temperature and humidity patterns, while their effect on velocity was less marked. They investigated both insulated and non-insulated spray chambers and reported that the insulation of a spray chamber will affect the airflow patterns, thereby affecting the droplet trajectories.

The modeling of spray dryers using the population balance method is gaining importance as the model accounts for droplet growth, coalescence and break up during the spray drying process. Nijdam et al. (2004) modeled the particle agglomeration within the spray chamber using two different frameworks, namely, Lagrangian and Eulerian. They validated their prediction using phase doppler anemometry (PDA) measurement, and found that in terms of ease of implementation and range of applicability, the Lagrangian approach is more suitable for modeling of agglomeration of particles. The modeling of droplet drying in the spray drying chamber by applying the unsteady mode of calculations (Mezhericher et al. 2009) showed that among 2D and 3D analyses, the latter predicts asymmetry of flow patterns in the spray chamber. Chen and Jin (2009b) performed transient 3D simulations in an industrial-scale spray dryer (15 m tall and 10 m wide). They observed that the particles make the central jet oscillate more non-linearly and that the frequency of oscillation decreases with increasing feed rate. Woo et al. (2009) have performed unsteady state simulations of spray drying and investigated the effect of chamber aspect ratio and operating conditions on flow stability. The authors observed that a large expansion ratio produces a more stable flow due to the limitations of jet fluctuations by outer geometry constriction.

2.12 Scope for Future Research

There remains scope for future research in the area of optimization of the spray drying process. Further work is needed to refine the turbulence models for the Lagrangian approach, in order to account for the various particle turbulence phenomena and particle–particle correlations. Modeling of particle agglomeration (including gas–particle interaction and particle–particle correlations), wall deposition (including nature of the product) and predicting particle residence time (including sliding movement of particles in the secondary residence time) during spray drying of food products is currently lacking. Hence, there is also scope for further study in the area to overcome problems like agglomeration, wall deposition, particle residence time, thermal degradation of particles and aroma loss (Kuriakose and Anandharamakrishnan 2010). Langrish (2007) has reported the same. Thus, the modeling approach may lead to better productivity and high-quality food products.

http://www.springer.com/978-1-4614-7989-5

Computational Fluid Dynamics Applications in Food Processing

Anandharamakrishnan, C.

2013, XI, 86 p. 36 illus., 24 illus. in color., Softcover
ISBN: 978-1-4614-7989-5